IEEE Access
Multidisciplinary ⋮ Rapid Review ⋮ Open Access Journal

Received 14 September 2025, accepted 5 October 2025, date of publication 8 October 2025, date of current version 14 October 2025.

Digital Object Identifier 10.1109/ACCESS.2025.3619396

RESEARCH ARTICLE

Integrated Biomechanical Motion Analysis in a Virtual Cycling Environment Using Wearable Sensors

ALEŠ PROCHÁZKA[1,2], (Life Senior Member, IEEE), HANA CHARVÁTOVÁ[3], MICHAELA HONZÍRKOVÁ[4], AND MARTIN SCHÄTZ[1]

[1]Department of Mathematics, Informatics and Cybernetics, University of Chemistry and Technology, Prague, 160 00 Prague, Czech Republic
[2]Czech Institute of Informatics, Robotics and Cybernetics, Czech Technical University in Prague, 160 00 Prague, Czech Republic
[3]Faculty of Applied Informatics, Tomas Bata University in Zlín, 760 01 Zlín, Czech Republic
[4]Department of Dermatovenerology, Motol University Hospital, 140 59 Prague, Czech Republic

Corresponding author: Aleš Procházka (A.Prochazka@ieee.org)

This work was supported in part by EU under the Project ROBOPROX in the area of Machine Learning under Grant CZ.02.01.01/00/22_008/0004590; in part by the Operational Program Johannes Amos Comenius financed by European Structural and Investment Funds and Czech Ministry of Education, Youth and Sports under Project SENDISO—CZ.02.01.01/00/22_008/0004596 in the area of data acquisition.

This work involved human subjects or animals in its research. Approval of all ethical and experimental procedures and protocols was granted by the Ethics Committee of the Neurological Center at Rychnov nad Kněžnou, Czech Republic.

ABSTRACT Biomechanical motion analysis in a virtual cycling environment through the inertial measurement units (IMU) forms a specific approach to movement assessment, integrating accelerometric and gyrometric sensors. The paper provides comprehensive data for evaluating physical activity, monitoring rehabilitation exercises, assessing neurological conditions, and detecting cardiological abnormalities. The dataset comprises 50 experiments and recordings from five distinct virtual cycling tours with varying altitude profiles, collectively spanning over 1,100 kilometers. The proposed methodology includes automated segmentation of cycling routes based on slope variation, extraction of statistical and frequency features from physiological, accelerometric, and gyrometric signals, and their subsequent classification using signal processing and computational intelligence techniques. Analysis of 3,526 segmented intervals revealed significant correlations between heart rate variations and slope gradients, as well as estimations of motion symmetry coefficients relevant to biomechanical assessment. The classification accuracy reached 95.5% for motion and physiological features, and 85.6% for gyrometric data using the two-layer neural network model across different slope conditions. The findings demonstrate the potential of hybrid systems combining wearable sensors and virtual environments for advanced motion analysis. This work underscores the applicability of general-purpose digital signal processing methods and machine learning algorithms in the multichannel analysis of physiological data, with applications in neurology, rehabilitation, and telemedicine.

INDEX TERMS Virtual cycling, computational intelligence, biomechanical motion analysis, wearable sensors, accelerometers, physical activity monitoring, detecting neurological disorders, rehabilitation.

I. INTRODUCTION

Analysis of motion patterns forms a broad research area essential for the detection of neurological disorders, monitoring of physical activities, evaluation of rehabilitation exercises [1], [2], and assessment of sports achievements [3], [4]. Data for mathematical analysis can be recorded in natural or hybrid environments. The present paper utilizes a virtual cycling platform (such as TACX, Zwift, or Wahoo), which enables exercises to be performed under conditions closely resembling real-world scenarios [5], [6], [7]. Additional sensors, including accelerometers, gyrometers [8], [9], [10], [11], and heart rate (HR) monitors [12], [13], can be integrated to form hybrid systems that facilitate

The associate editor coordinating the review of this manuscript and approving it for publication was Ramoni Adeogun.

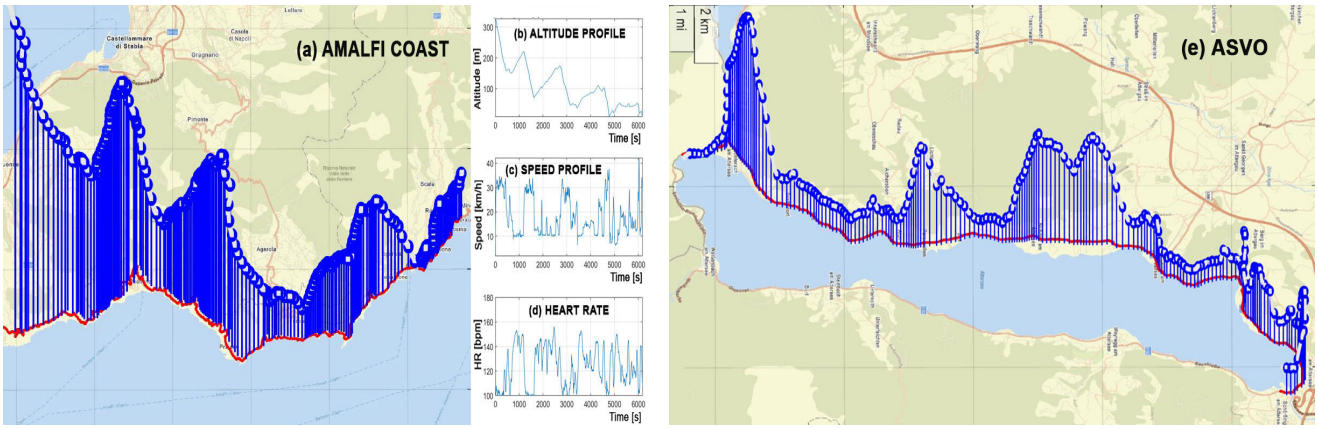

FIGURE 1. Selected routes for virtual cycling data analysis, presenting (a) three-dimensional profile of the Amalfi coast cycling virtual tour with the mapping environment, (b,c,d) associated signals presenting the altitude profile, speed, and heart rate, and (e) three-dimensional profile of the Asvo route around the Attersee lake acquired during virtual cycling using the TACX smart trainer system for motion analysis at segments with different slopes.

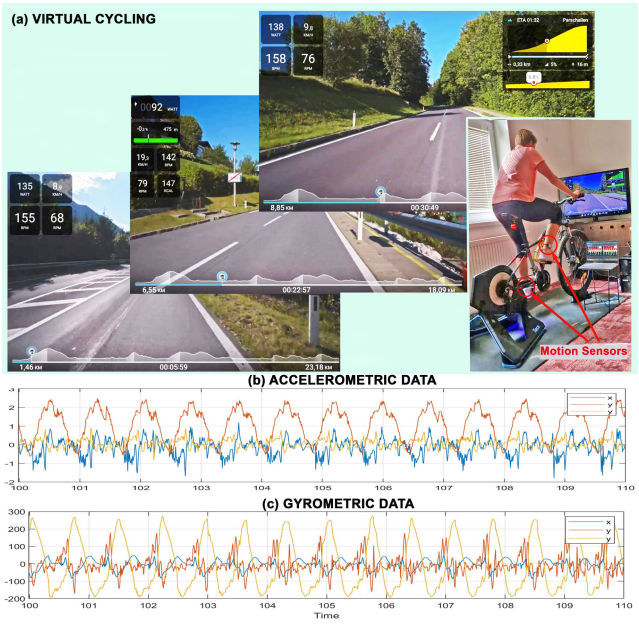

FIGURE 2. The set of images from the video record of the Asvo route around the Attersee lake acquired during virtual cycling using the TACX smart trainer system, presenting (a) virtual cycling, (b) a sample of accelerometric, and (c) gyrometric data.

the acquisition of signals for a more detailed analysis of biomechanics, posture, and muscle engagement. Such time-synchronized, multichannel systems can be processed using general digital signal processing (DSP) techniques [14], supported by computational and artificial intelligence (AI) methods [15], [16].

An extensive research is devoted to the use of inertial measurement units (IMU) in the study of human kinematics and kinetics [17], [18]. These studies present results for different positions of IMU sensors [19], [20] on the neck, thorax, pelvis, hip, knee, and ankle for data acquisition in many cases. The methodologies of data processing include the use of digital signal processing and artificial intelligence applications for noise suppression, activity recognition, symmetry detection, machine learning, and classification. Specific case studies demonstrate a virtual reality (VR) environment combined with wearable sensors. A wide range of applications in neurology and rehabilitation [21] is devoted to the detection of neurologic disorders, studies of similarities between the muscle synergies during walking and pedaling, monitoring of rehabilitation exercises, and evaluation of the fitness level.

Rapid technological progress enables the use of sophisticated wearable sensors that can record accelerometric, gyrometric, depth, thermal, visual, and positioning signals and images for data acquisition. Interdisciplinary computational and AI methods can then be applied to motion analysis [22], [23] in the time, frequency, and scale domains to detect motion features associated with various external conditions and the individual's fitness level, supporting the classification of motion habits and potential motion disorders. Deep learning techniques often integrate pose estimation with signal processing methods [24].

Inertial measurement units provide motion performance indicators [27] that are important for tracking cyclists and assessing their fitness levels, as well as for monitoring physiological functions [28], including heart rate responses under various environmental conditions. They are also valuable for detecting movement disorders relevant to neurology [29], brain health [30], and mental dysfunctions [31]. Numerous research studies focus on capturing biomechanics [32], [33], [34] in clinical and laboratory settings to enhance motion performance and reduce the risk of injury [35].

This paper is based on data acquired using a home smart trainer [25], [26], which enables data collection during virtual routes, as presented in Fig. 1, projected on a screen in front of the individual. The cycling load is determined by the route profile, allowing for the acquisition of data closely resembling that recorded during real-world cycling experiments. Figure 2 presents a set of images from a video

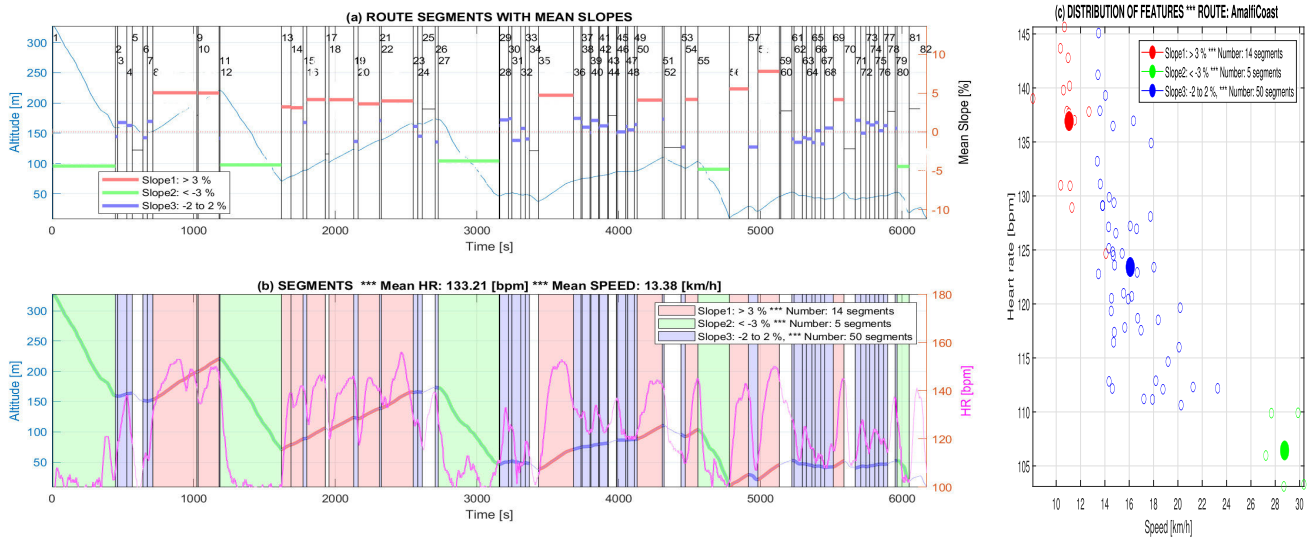

FIGURE 3. Results of segmentation of the selected Amalfi Coast virtual cycling tour, presenting (a) route segments with three different route slopes with their boundaries detected as local extrema of the altitude signal, (b) global statistics of the route with the numbers of segments belonging to specified mean slope values, and (c) distribution of selected features, including the speed and the heart rate related to different slopes acquired during one experiment of virtual cycling.

recording of the selected virtual route, along with a sample of the corresponding accelerometric and gyrometric data collected during the virtual cycling experiment.

The goal of this study is in investigation of (i) multichannel motion and physiological data acquisition, (ii) segmentation of real routes into regions with selected average slopes, (iii) analysis of mean heart rate during virtual cycling, and (iv) detection of features within each segment and their classification using machine learning tools. The following parts of the paper include Section II with a description of the data acquisition system and general methods of data processing, Section III with results of specific experiments, Section IV discussing results, and Section V with conclusions.

Algorithm 1 Altitude Data Segmentation

1) Altitude data resampling using spline interpolation and time-stamps with the sampling period of 0.5 seconds.
2) Digital filtering using median and the FIR filter of the 60th order and the cutoff frequency of 0.35 Hz.
3) The detection of local maximum and minimum altitudes not closer than 60 seconds for specification of data segments.
4) Evaluation of mean slopes in separate segments as the ratio of altitude data differences and the sampling period.
5) Detection of segments in 3 slope categories of steep uphill, steep downhill, and flat surface cycling for further analysis.

II. METHODS

A. DATA ACQUISITION

Virtual cycling was performed on a bicycle mounted on a TACX Neo 2T smart trainer, which recorded virtual cycling position, speed, and distance during the exercise without demands for system calibration but with the need of an Internet connection for virtual position specification. A Garmin system measured the subject's heart rate, while WitMotion WT901SDCL-BT50 sensors recorded acceleration and angular velocity after their calibration at a sampling frequency of 100 Hz. Figure 2 shows a set of images and a sample of motion data recorded during a virtual ride around Lake Attersee, acquired using the TACX smart trainer system.

The selected routes used for virtual cycling data analysis are shown in Fig. 1. Figures 1(a–d) depict a three-dimensional profile of the Amalfi Coast virtual cycling tour, including the map environment and associated signals, such as altitude profile, speed, and heart rate. Figure 1(e) displays the profile of the Asvo route around Lake Attersee, acquired during a virtual cycling session.

The dataset includes analysis of 50 experimental runs and data recorded during 5 selected tours with varying altitude profiles, collectively forming a cycling route of over 1,100 km. The multichannel signals comprise data recorded by the TACX device and a heart rate sensor. Motion sensors were connected via the WitMotion desktop application.

Selected signals are available on IEEE DataPort (DOI: 10.21227/dgap-pq18, Virtual Cycling Tours) [36] and Zenodo repository (10.5281/zenodo.17069366) for further investigation. These repositories contain signals acquired by the TACX Neo 2T smart trainer, motion data, and heart rate sensors in tabular forms with associated time-stamps.

Algorithm 2 Motion Data Classification

1) Definition of pattern matrix with the mean speed and mean heart rate for each segment and associated target vector that defines class 1 (steep uphill), 2 (steep downhill), and 3 (flat surface).
2) Evaluation of pattern matrix with the mean energy in the given range of the left and right legs for each segment and associated target vector that defines classes 1, 2, and 3.
3) Statistical analysis that specifies mean values and standard deviation of data of each class and removal of patterns and targets outside the given limits.
4) Detailed classification of cycling patterns using machine learning and specific methods, including neural networks.
5) Estimation of accuracies and cross-validation errors of selected classification methods.

B. DATA PROCESSING METHODOLOGY

Data processing methods depend on the signal features and the characteristics of the sensors used for data acquisition. The database compiled from the present virtual cycling experiments includes multichannel, time-synchronized signals consisting of accelerometric, gyrometric, heart rate, longitude, latitude, altitude, and speed data, all associated with corresponding time-stamps.

Statistical analysis of the positioning signals was employed to perform the fundamental route profile analysis. The initial step in signal processing for each experiment involved segmenting the route according to the altitude profile and the detection of its local extremal values. Fundamental mathematical and computational steps are summarized in Algorithm 1 for classification into 3 classes. This process was applied for each route and repetitive exercises, as illustrated in Fig. 3. The selection of a minimum peak distance (60 seconds in this case) determined the minimum segment length along the route. The resulting time series $s(l,n)_{n=0}^{N-1}$ for each route segment l included heart rate, speed, and positioning data.

Individual accelerometric and gyrometric signals were recorded using tri-axial sensors attached to the left and right legs above the ankles. These data generated three signal sequences $s_x(l,n), s_y(l,n), s_z(l,n)_{n=0}^{N-1}$ for both accelerometric ($l=1$) and gyrometric ($l=2$) measurements. Preprocessing included median filtering of a selected order, followed by FIR digital filtering to remove noise components from the signals.

Further processing included processing of separate motion data components and analysis of their modulus, calculated by the following relation:

$$s(l,n) = \sqrt{s_x(l,n)^2 + s_y(l,n)^2 + s_z(l,n)^2} \tag{1}$$

with their mean value $\bar{s}(l) = \sum_{n=0}^{N-1} s(l,n)/N$. Spectral components of these signals were then evaluated by the discrete Fourier transform:

$$S(l,k) = \sum_{n=0}^{N-1} (s(l,n) - \bar{s}(l))\, e^{-j\,k\,n\,2\,\pi/N} \tag{2}$$

for $k = 0, 1, \cdots, N-1$. Frequency domain features were then calculated as the relative power $E_p(l,d)$ for each data segment $d = 1, 2, \cdots, Q$ in the frequency band $\langle fc_1, fc_2 \rangle$ for each position p of the sensor and route segment l by relation:

$$E_p(l,d) = \frac{\sum_{k\in\Phi_w} |S(l,k)|^2}{\sum_{k=0}^{N/2} |S(l,k)|^2} \tag{3}$$

where Φ_w denotes the set of indices for the spectral components within the selected frequency range $\langle fc_1, fc_2 \rangle$.

Values of relative energy for both the left and right sides of the body were used for the estimation of motion symmetry and evaluation of motion features used for classification. The motion symmetry was estimated as the ratio of energy for the left and right sides of the body by relation:

$$C(d) = \frac{E_{Left}(l,d)}{E_{Right}(l,d)} \tag{4}$$

for each data segment d.

Frequency domain motion features estimated for both the left and right sides of the body and accelerometric ($l=1$) and gyrometric ($l=2$) data were then used for construction of the pattern matrix

$$P_l = \begin{bmatrix} E_{Left}(l,1) & \cdots & E_{Left}(l,Q) \\ E_{Right}(l,1) & \cdots & E_{Right}(l,Q) \end{bmatrix} \tag{5}$$

and target vector T that associated each feature column vector of matrix P_l with class s_k that specified the slope for the following classification.

Mean values and standard deviations of features associated with individual classes were used for the rejection of gross errors and the removal of associated columns of matrix P_l and vector T. Values within a selected vicinity of centres of gravity of individual classes were used for further processing.

The selection of frequency ranges for the evaluation of features was based upon class separability metric [37] associated with features evaluated for uphill cycling (with the mean slope above 3%) and downhill cycling (with the mean slope bellow −3%). Individual classes with their centres of gravity were specified by

1) the inter-class Euclidean distance $dist(l)_{mean}$ between their mean values,
2) the average within-class variability estimated as the mean of the standard deviations $\sigma(l)_{mean}$ of distances between individual patterns locations and associated class centres of gravity.

Class separability ratio SR was then evaluated as

$$SR(l) = \frac{dist(l)_{mean}}{\sigma(l)_{mean}} \tag{6}$$

for accelerometric ($l=1$) and gyrometric ($l=2$) data. A higher SR means better separation between the two classes

TABLE 1. Percentage of excluded features of slope *S1* (> 3%) and slope *S2* (< −3%) for selected multiples of standard deviations for five routes, selected frequency ranges, and features of accelerometric, gyrometric and motion (heart rate [bpm] and speed [km/h]) data.

Route	Frequency Range [Hz]	Percentage of excluded features					
		Accelerometry		Gyrometry		HR/speed	
		S1	S2	S1	S2	S1	S2
1	0.5 to 10.0	0.0	0.0	5.2	7.7	0.0	0.0
	0.5 to 5.0	0.0	0.0	19.0	15.4		
	0.8 to 2.5	1.7	0.0	15.5	15.4		
	1.5 to 4.0	1.7	3.8	8.6	11.5		
2	0.5 to 10.0	1.4	2.0	10.8	5.9	0.0	0.2
	0.5 to 5.0	1.4	2.0	10.1	5.9		
	0.8 to 2.5	0.7	2.0	16.2	11.8		
	1.5 to 4.0	2.0	2.0	11.5	17.6		
3	0.5 to 10.0	0.0	0.0	14.1	7.7	0.0	0.0
	0.5 to 5.0	0.0	0.0	15 2	7.7		
	0.8 to 2.5	2.2	0.0	15.2	7.7		
	1.5 to 4.0	3.3	0.0	14.1	23.1		
4	0.5 to 10.0	1.6	0.0	15.9	14.5	0.0	0.0
	0.5 to 5.0	0.0	0.0	11.1	8.1		
	0.8 to 2.5	0.0	0.0	6.4	3.2		
	1.5 to 4.0	1.6	1.6	14.3	6.5		
5	0.5 to 10.0	0.0	0.0	14.9	5.6	0.0	0.0
	0.5 to 5.0	0.0	0.0	18.1	11.1		
	0.8 to 2.5	1.7	0.0	14.9	16.7		
	1.5 to 4.0	1.1	5.6	10.6	10.1		
All12345	0.5 to 10.0	4.2	0.6	9.2	10.0	0.4	0.0
	0.5 to 5.0	3.1	0.6	15.4	14.1		
	0.8 to 2.5	3.5	1.2	14.9	13.5		
	1.5 to 4.0	0.9	2.9	10.8	11.2		

(relative to spread). This metric is similar to the Fisher criterion used in linear discriminant analysis.

Machine learning and computational intelligence methods were further applied. During the learning process, a function that transforms the space of features P_l into the vector T specifying the classes, both for accelerometric and gyrometric data, is estimated. The final classification was performed by Bayesian and support vector machine model. Results were then compared with the two-layer neural model using 80% of data for training, 10% for validation, and 10% for testing.

The evaluation of classification results involved analyzing the two-class receiver operating characteristic (ROC) based on the number of true positives TP, false negatives FN, false positives FP, and false negatives FN. The ROC analysis is used to calculate the accuracy, defined as the proportion of total correct predictions (both true positives and true negatives) out of all predictions made by the model, providing an overall measure of how well the model performs across both classes:

$$AC = \frac{TP + TN}{TP + TN + FP + FN} \tag{7}$$

Verification was done by the evaluation of the 10-fold cross-validation error that assumes splitting of the whole set into 10 subsets (folds) and the evaluation of errors for each fold using a model trained for other 9 folds. The 10-fold cross-validation error is then calculated as their average.

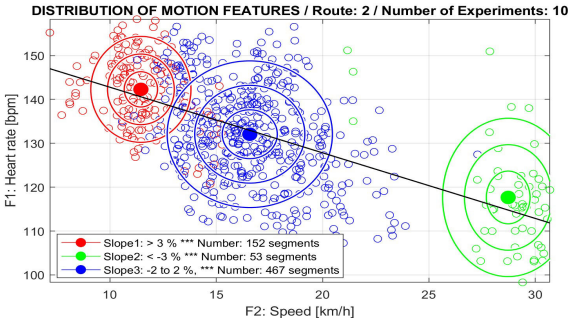

FIGURE 4. Distribution of selected features, including the speed and the heart rate related to different slopes acquired during ten experiments of virtual cycling on the Amalfi Coast with *m*-multiples of standard deviations (for *m* =0.5,1,1.5).

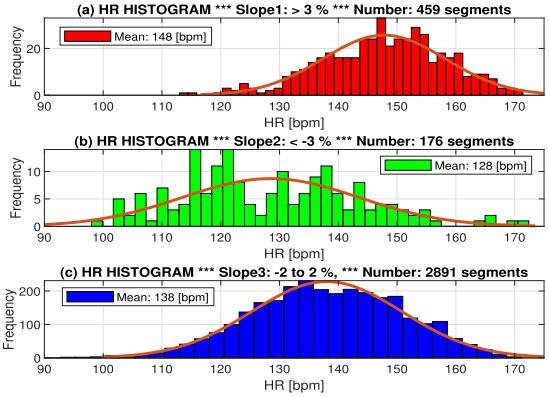

FIGURE 5. Distribution of the heart rate values related to different slopes acquired during exercises on five routes with ten experiments of virtual cycling on each of them.

TABLE 2. Mean values of the heart rate [bpm] for virtual cycling on Slope1 (> 3%), Slope2 (< −3%), and Slope3 (> −2% & < 2%) for five routes.

Route	Mean Heart Rate [bpm]		
	Slope1	Slope2	Slope3
1	146	141	139
2	152	116	132
3	153	138	142
4	148	130	138
5	152	130	139
All12345	150	131	138

Fundamental signal processing steps that followed data segmentation are summarized in Algorithm 2.

III. RESULTS

Data acquisition was performed using accelerometric, gyrometric, speed, and heart rate signals using the methodology summarized in Algorithms 1 and 2.

Figure 3 shows the results of segmenting the selected Amalfi Coast virtual cycling tour into three different route slopes. It also presents global statistics of the route, including the number of segments and the distribution of selected features—such as speed and heart rate—associated with the different slopes, based on one virtual cycling experiment.

TABLE 3. Separability index of Slope1 (> 3%) and Slope2 (< −3%) for five routes and their combination for selected frequency ranges for accelerometric, gyrometric and motion (heart rate HR [bpm] and speed [km/h]) data with its highest value for each route and their combination.

Route	Frequency range [Hz]	Separability Ratio		
		Acelerometry	Gyrometry	HR/speed
1	0.5 to 10.0	1.992	**3.041**	1.657
	0.5 to 5.0	2.154	0.803	
	0.8 to 2.5	**2.493**	2.447	
	1.5 to 4.0	1.355	0.070	
2	0.5 to 10.0	2.196	**1.764**	6.085
	0.5 to 5.0	**2.249**	0.043	
	0.8 to 2.5	1.951	1.577	
	1.5 to 4.0	1.191	0.803	
3	0.5 to 10.0	**0.726**	0.887	4.712
	0.5 to 5.0	0.371	0.733	
	0.8 to 2.5	0.114	**1.343**	
	1.5 to 4.0	0.542	1.102	
4	0.5 to 10.0	1.858	**1.251**	3.836
	0.5 to 5.0	**2.216**	0.291	
	0.8 to 2.5	2.059	1.237	
	1.5 to 4.0	0.990	0.074	
5	0.5 to 10.0	1.364	1.436	4.434
	0.5 to 5.0	1.677	0.954	
	0.8 to 2.5	**2.134**	**2.334**	
	1.5 to 4.0	0.957	0.511	
All12345	0.5 to 10.0	1.114	1.405	3.304
	0.5 to 5.0	1.273	0.691	
	0.8 to 2.5	**1.317**	**1.705**	
	1.5 to 4.0	0.465	0.438	

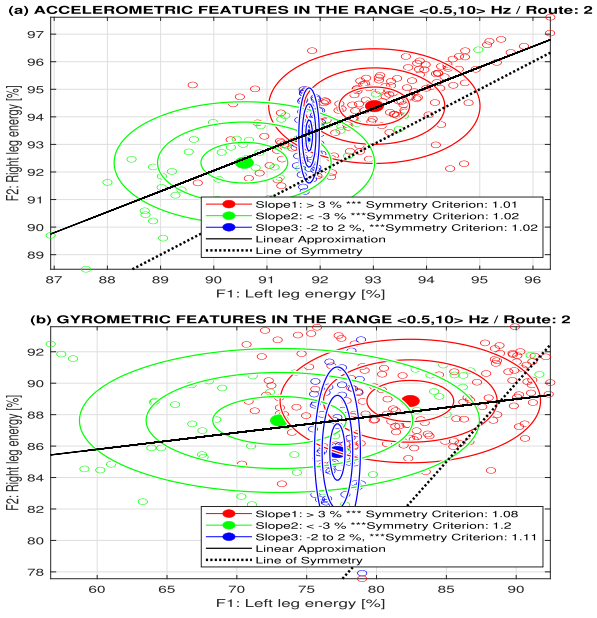

FIGURE 6. Distribution of (a) accelerometric and (b) gyrometric frequency features of virtual cycling on the Amalfi Coast and ten virtual cycling experiments with means of separate clusters and *m*-multiples of standard deviations (for m =0.5,1,1.5).

Table 1 presents the percentage of excluded features for slope $S1$ (greater than 3%) and slope $S2$ (less than −3%) across five routes and selected frequency ranges for accelerometric, gyrometric, and motion data (heart rate [bpm] and speed [km/h]). Feature ranges were defined around the mean values for each slope. Segments with

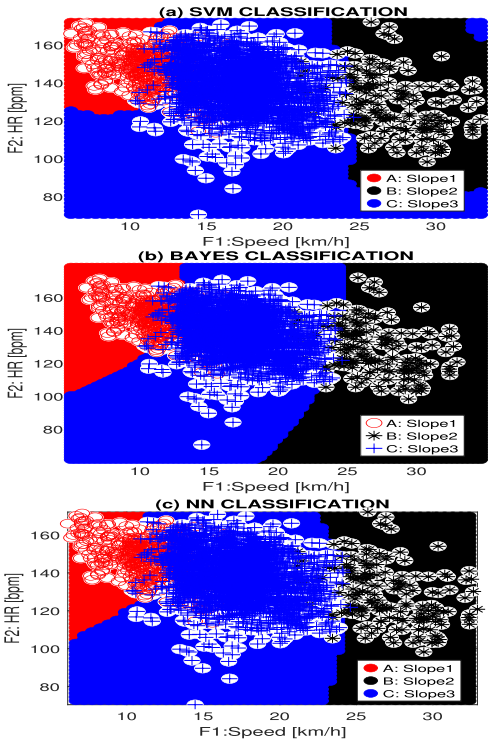

FIGURE 7. Classification of heart rate and speed features by (a) the support vector machine (SVM), (b) Bayes, and (c) neural network (NN) method using features of virtual cycling on five cycling routes and ten virtual cycling experiments for each of them.

TABLE 4. Results of classification by the support vector machine (SVM), Bayes method, and the two layer neural network (NN) comparing accuracy and cross-validation (CV) values for the full and reduced data sets with the highest values in bold.

Data	Classification of the Full Data Set					
	SVM		Bayes		NN	
	ACC	CV	ACC	CV	ACC	CV
HR/Speed	94.6	5.7	93.7	6.1	**94.7**	5.6
Accelerometry	82.2	15.9	82.0	18.5	**82.6**	16.6
Gyrometry	82.4	18.7	81.5	18.7	**82.4**	17.6
	Classification of the Reduced Data Set					
HR/Speed	94.8	5.6	93.9	6.1	**95.5**	5.0
Accelerometry	82.2	16.6	82.6	16.6	**83.7**	15.6
Gyrometry	83.1	18.0	83.2	16.7	**85.8**	14.7

their values greater or lower than the mean $\pm c$-multiple of standard deviations were removed, using c =3 for accelerometric and speed data, and c =1.5 for gyrometric data. Due to the more compact clustering of accelerometric data, on average only 2% were excluded, compared to 12% of gyrometric data excluded across all frequency ranges.

Figure 4 shows the distribution of heart rate and speed at different slopes, based on ten virtual cycling experiments on the Amalfi Coast. The feature clusters are well separated, with their centers of gravity aligning closely along a well-defined approximation line. Figure 5 presents the distribution of heart rate values associated with different slopes, collected from exercises on five

routes, each with ten virtual cycling experiments. For a total of 3,526 segments—after removing gross errors—mean heart rate values during virtual cycling on three selected slope categories were evaluated. The mean heart rate values [bpm] for Slope1 (> 3%), Slope2 (< −3%), and Slope3 (between −2% and 2%) across five routes are presented in Table 2. These results are consistent with recent research on heart rate variability in cyclists [25], [38], [39], [40].

Table 3 presents separability indices for Slope1 (> 3%) and Slope2 (< −3%) across five routes, as well as their combined values, for selected frequency ranges of accelerometric, gyrometric, and motion data (heart rate [bpm] and speed [km/h]). The highest separability value for each route and the overall combination is also highlighted. The separability ratio is influenced by the route profile, with the highest value of 3.041 observed for Route 1 using gyrometric data.

Figure 6 illustrates the distribution of accelerometric and gyrometric frequency features from ten virtual cycling experiments on the Amalfi Coast. Frequency features estimated for the left and right legs were evaluated by Eq. (5) and the frequency band $\langle fc_1, fc_2 \rangle$ Hz. The selection of frequency limits of fc_1 =0.5 and fc_2 =10 Hz was based on the highest separability index and results in Table 3. The gravity centers of the individual clusters are positioned near the approximation line, all located above the axis of symmetry. This observation suggests a slightly asymmetric motion pattern of the individual performing the exercise.

Figure 7 presents the classification of heart rate and speed features by the support vector machine (SVM), Bayes, and neural network (NN) method, over all five routes and ten virtual cycling experiments, processing 3,526 segments and dividing them into three clusters with different slopes.

Table 4 presents the results of classifying heart rate, speed, accelerometric, and gyrometric signal features using support vector machines, the Bayes method, and a two-layer neural network for the full set of 3,526 segments and the reduced set of 2,891 segments. The comparison of accuracy and cross-validation values indicates that the neural network classification model achieved the highest performance. The removal of outliers increased the accuracy and decreased the cross-validation errors.

IV. DISCUSSION

Inertial sensors for human motion analysis are widely used to monitor physical performance and everyday movement in both home and clinical environments. Their multidisciplinary applications often integrate machine learning techniques and biomechanical modelling.

This paper focuses on analysis of motion patterns during virtual cycling across various routes. The proposed experimental setup can serve as a valuable tool for assessing fitness levels, detecting motion disorders, evaluating the risk of cardiovascular diseases, and monitoring rehabilitation exercises. Differences in spectral components between the left and right legs during motion may indicate neuromuscular disorders (including Parkinson's disease), walking asymmetries [2], and sport activities level (including alpine skiing [41]).

Limitations of the proposed method include the necessity of using the smart trainer, wearable sensors, and communication links for data acquisition. Further limitations given by the use of Matlab computational environment can be eliminated by the proposal of the associated web page. Additional potential problems include the use of intelligent methods for the reduction of sensor noise and participants' variability.

Artificial intelligence can assist in identifying improper movement patterns during cycling and can be applied in both professional training and rehabilitation contexts. This paper is based upon selected motion features, while progress of deep learning will allow using all raw data and elimination of frequency bands selection in case of large enough datasets.

V. CONCLUSION

The present paper follows current trends in the sophisticated use of wearables, machine learning, and multidisciplinary applications of digital signal processing. Its specific contribution is in the presentation of the virtual environment that can replace real-world exercises and provide similar data for evaluation of the fitness level and estimation of motion disorders of individuals.

Future research will focus on more advanced computational intelligence techniques for analyzing signals collected during virtual cycling. Special attention will be paid to deep learning, evaluation of an extensive set of individuals, and scalability of the population. Digital twin models of cyclists hold another significant potential for simulating physiological and musculoskeletal responses to personalized virtual rides, as well as for finding motion anomalies, and early detection of neurodegenerative conditions. Specific studies will include proposals of exercises appropriate for monitoring neurological disorders, rehabilitation, and fitness level improvements.

REFERENCES

[1] Y. Jiao, W. Wang, J. Wang, and Z.-G. Hou, "Proprioception enhancement for robot assisted neural rehabilitation: A dynamic electrical stimulation based method and preliminary results from EEG analysis," *J. Neural Eng.*, vol. 21, no. 4, Aug. 2024, Art. no. 046043.

[2] L. Gonsorčíková, A. Procházka, A. Molčanová, D. Janáková, M. Honzírková, H. Charvátová, L. Šímová, and O. Vyšata, "Assessing pediatric gait symmetry through accelerometry and computational intelligence," *IEEE Access*, vol. 12, pp. 125358–125368, 2024.

[3] J. E. Morais, J. A. Bragada, P. M. Magalhães, and D. A. Marinho, "The accuracy and reliability of the power measurements of the TACX neo 2T smart trainer and its agreement against the garmin vector 3 pedals," *J. Funct. Morphology Kinesiol.*, vol. 9, no. 3, p. 138, Aug. 2024.

[4] A. Silacci, R. Taiar, and M. Caon, "Towards an AI-based tailored training planning for road cyclists: A case study," *Appl. Sci.*, vol. 11, no. 1, p. 313, Dec. 2020.
[5] M. Bogacz, S. Hess, C. F. Choudhury, C. Calastri, F. Mushtaq, M. Awais, M. Nazemi, M. A. B. van Eggermond, and A. Erath, "Cycling in virtual reality: Modelling behaviour in an immersive environment," *Transp. Lett.*, vol. 13, no. 8, pp. 608–622, Sep. 2021.
[6] A. Rojo, R. Raya, and J. C. Moreno, "Virtual reality application for real-time pedalling cadence estimation based on hip ROM tracking with inertial sensors: A pilot study," *Virtual Reality*, vol. 27, no. 1, pp. 3–17, Mar. 2023.
[7] L. Poli, G. Greco, M. Gabriele, I. Pepe, C. Centrone, S. Cataldi, and F. Fischetti, "Effect of outdoor cycling, virtual and enhanced reality indoor cycling on heart rate, motivation, enjoyment and intention to perform green exercise in healthy adults," *J. Funct. Morphology Kinesiol.*, vol. 9, no. 4, p. 183, Oct. 2024.
[8] A. Cereatti, R. Gurchiek, A. Mündermann, S. Fantozzi, F. Horak, S. Delp, and K. Aminian, "ISB recommendations on the definition, estimation, and reporting of joint kinematics in human motion analysis applications using wearable inertial measurement technology," *J. Biomechanics*, vol. 173, Aug. 2024, Art. no. 112225.
[9] A. Procházka, H. Charvátová, O. Vyšata, D. Jarchi, and S. Sanei, "Discrimination of cycling patterns using accelerometric data and deep learning techniques," *Neural Comput. Appl.*, vol. 33, no. 13, pp. 7603–7613, Jul. 2021.
[10] I. I. Savio Gunawan, Y. Gu, I. Goncharenko, and S. Kamijo, "Cyclist speed estimation using accelerometer and gyroscope in smartphones," in *Proc. IEEE 4th Global Conf. Life Sci. Technol. (LifeTech)*, Mar. 2022, pp. 441–442.
[11] M. Arias-Correa, S. Robledo, M. Londoño, J. Mejía, C. A. Madrigal-González, J. R. Ballesteros, and J. W. Branch, "CYCLOPS: A cyclists' orientation data acquisition system using RGB camera and inertial measurement units (IMU)," *HardwareX*, vol. 18, Jun. 2024, Art. no. e00534.
[12] P. S. Kasiak, S. Wiecha, I. Cieslinski, T. Takken, J. Lach, M. Lewandowski, M. Barylski, A. Mamcarz, and D. Sliz, "Validity of the maximal heart rate prediction models among runners and cyclists," *J. Clin. Med.*, vol. 12, no. 8, p. 2884, Apr. 2023.
[13] A. Nazaret, S. Tonekaboni, G. Darnell, S. Y. Ren, G. Sapiro, and A. C. Miller, "Modeling personalized heart rate response to exercise and environmental factors with wearables data," *npj Digit. Med.*, vol. 6, no. 1, pp. 207:1–207:7, Nov. 2023.
[14] A. Procházka, O. Vyšata, and V. Mařík, "Integrating the role of computational intelligence and digital signal processing in education," *IEEE Signal Processing Magazine*, vol. 38, no. 3, pp. 154–162, 2021.
[15] C.-H. Ho, P. Qiu, Y. Zhang, and K. Ren, "A generic deep learning-based computing algorithm in support of the development of instrumented bikes," *ASCE OPEN, Multidisciplinary J. Civil Eng.*, vol. 2, no. 1, pp. 1–16, Dec. 2024.
[16] V. Vec, S. Tomažic, A. Kos, and A. Umek, "Trends in real-time artificial intelligence methods in sports: A systematic review," *J. Big Data*, vol. 11, no. 1, pp. 148:1–148:23, Oct. 2024.
[17] W. Liang, "Extended application of inertial measurement units in human kinematics and kinetics assessment," *Sensors*, vol. 23, no. 9, pp. 4229:1–4229:20, 2023.
[18] T. Caporaso, S. Grazioso, and G. Di Gironimo, "Development of an integrated virtual reality system with wearable sensors for ergonomic evaluation of human–robot cooperative workplaces," *Sensors*, vol. 22, no. 6, p. 2413, Mar. 2022.
[19] L. Winter, C. Bellenger, P. Grimshaw, and R. G. Crowther, "Analysis of movement variability in cycling: An exploratory study," *Sensors*, vol. 23, no. 10, p. 4972, May 2023.
[20] V. Kumar and D. K. Pratihar, "Wearable sensor-based intent recognition for adaptive control of intelligent ankle-foot prosthetics," *Measurement: Sensors*, vol. 39, Jun. 2025, Art. no. 101865.
[21] J. Tsuchiya, K. Momose, H. Saito, K. Watanabe, and T. Yamaguchi, "Comparison of muscle synergies in walking and pedaling: The influence of rotation direction and speed," *Frontiers Neurosci.*, vol. 18, pp. 1485066:1–1485066:12, Dec. 2024.
[22] S. Díaz, J. B. Stephenson, and M. A. Labrador, "Use of wearable sensor technology in gait, balance, and range of motion analysis," *Appl. Sci.*, vol. 10, no. 1, p. 234, Dec. 2019.
[23] A. Procházka, M. Schätz, O. Tupa, M. Yadollahi, O. Vysata, and M. Walls, "The MS Kinect image and depth sensors use for gait features detection," in *Proc. IEEE Int. Conf. Image Process. (ICIP)*, Oct. 2014, pp. 2271–2274.
[24] Y. He, Y.-H. Jan, F. Yang, Y. Ma, and C. Pei, "A novel method for assessing cycling movement status: An exploratory study integrating deep learning and signal processing technologies," *BMC Med. Informat. Decis. Making*, vol. 25, no. 1, pp. 71:1–71:11, Feb. 2025.
[25] H. Charvátová, D. Martynek, A. Molčanová, and A. Procházka, "Rehabilitation and motion symmetry analysis with a TACX smart cycling trainer using computational intelligence," *IEEE Access*, vol. 13, pp. 113495–113501, 2025.
[26] C. Supriyanto and B. Liu, "Virtual cycling for promoting a healthy lifestyle," *Int. J. Sci., Technol. Manage.*, vol. 2, no. 1, pp. 60–71, Jan. 2021.
[27] R. Thompson, R. Rico Bini, C. Paton, and K. Hébert-Losier, "Validation of LEOMO inertial measurement unit sensors with marker-based three-dimensional motion capture during maximum sprinting in track cyclists," *J. Sports Sci.*, vol. 42, no. 2, pp. 179–188, Jan. 2024.
[28] T. Lim, A. Kalra, J. Thompson, J. C. Odgers, and B. Beck, "Physiological measures of bicyclists' subjective experiences: A scoping review," *Transp. Res.*, vol. 90, pp. 365–381, Aug. 2022.
[29] I. B. S. Ferré, G. Corso, G. Z. dos Santos Lima, S. R. Lopes, M. A. Leocadio-Miguel, L. G. S. França, T. de Lima Prado, and J. F. Araujo, "Cycling reduces the entropy of neuronal activity in the human adult cortex," *PLoS ONE*, vol. 19, no. 10, Oct. 2024, Art. no. e0298703.
[30] C. Hou, Y. Zhang, F. Zhao, Y. Lv, M. Luo, C. Pan, D. Ding, and L. Chen, "Active travel mode and incident dementia and brain structure," *JAMA Netw. Open*, vol. 8, no. 6, Jun. 2025, Art. no. e2514316.
[31] B. B. Kramer, S. F. Højholt, D. Sørensen, L. U. Sørensen, and M. D. Terkildsen, "Virtual cycling as an exercise intervention in forensic psychiatry: A qualitative study," *Digit. HEALTH*, vol. 11, pp. 1–13, May 2025.
[32] W. Holliday and J. Swart, "A dynamic approach to cycling biomechanics," *Phys. Med. Rehabil. Clinics North Amer.*, vol. 33, no. 1, pp. 1–13, Feb. 2022.
[33] G. Millour, A. T. Velásquez, and F. Domingue, "A literature overview of modern biomechanical-based technologies for bike-fitting professionals and coaches," *Int. J. Sports Sci. Coaching*, vol. 18, no. 1, pp. 292–303, Feb. 2023.
[34] C. E. Clancy, A. A. Gatti, C. F. Ong, M. R. Maly, and S. L. Delp, "Muscle-driven simulations and experimental data of cycling," *Sci. Rep.*, vol. 13, no. 1, pp. 21534:1–21534:10, Dec. 2023.
[35] M. A. B. van Eggermond, D. Schaffner, N. Studer, L. Knecht, and L. Johnson, "Assessing the effectiveness of an online cycling training for adults to master complex traffic situations," *Accident Anal. Prevention*, vol. 211, Mar. 2025, Art. no. 107856.
[36] A. Procházka, H. Charvátová, T. Tumová, and O. Vyšata, "Virtual cycling tours," IEEE Dataport, Piscataway, NJ, USA, Jul. 15, 2025, doi: 10.21227/dgap-pq18.
[37] M. Shamsi and S. Beheshti, "Separability and scatteredness (S&S) ratio-based efficient SVM regularization parameter, kernel, and kernel parameter selection," *Pattern Anal. Appl.*, vol. 28, no. 1, pp. 33:1–33:13, Mar. 2025.
[38] P. Hebisz, R. Hebisz, and A. Jastrzebska, "An attempt to predict changes in heart rate variability in the training intensification process among cyclists," *Int. J. Environ. Res. Public Health*, vol. 18, no. 14, p. 7636, Jul. 2021.
[39] S. Le Douairon Lahaye, G. Kervio, V. Menard, A. Barrero, T. Lachard, G. Carrault, D. Matelot, F. Carré, and F. Schnell, "Impact of long-lasting moderate-intensity stage cycling event on cardiac function in young female athletes: A case study," *PLoS ONE*, vol. 17, no. 10, Oct. 2022, Art. no. e0275332.
[40] R. P. Lamberts, T. van Erp, A. Javaloyes, M. M. Eken, N. G. Langerak, and N. Tam, "Reliability of recovery heart rate variability measurements as part of the lamberts submaximal cycle test and the relationship with training status in trained to elite cyclists," *Eur. J. Appl. Physiol.*, vol. 124, no. 6, pp. 1659–1668, Jun. 2024.
[41] A. Procházka and H. Charvátová, "Wearable sensors and computational intelligence in Alpine skiing analysis," *IEEE Access*, vol. 13, pp. 70414–70421, 2025.

ALEŠ PROCHÁZKA (Life Senior Member, IEEE) received the Ph.D. degree, in 1983. He was appointed as a Professor of technical cybernetics with Czech Technical University in Prague (CTU), Prague, in 2000. He is currently the Head of the Digital Signal and Image Processing Research Group with the Department of Mathematics, Informatics and Cybernetics, UCT, and Czech Institute of Informatics, Robotics and Cybernetics, CTU. His research interests include mathematical methods of multidimensional data analysis, segmentation, feature extraction, classification, and modelling in biomedicine and engineering. He is a member of IET and EURASIP. He has served as an Associate Editor for Signal, Image and Video Processing (Springer). He is a reviewer for different IEEE, Springer, and Elsevier journals.

HANA CHARVÁTOVÁ received the Ph.D. degree in chemistry and materials technology with the Faculty of Technology, TBU, Zlín, for the Technology of Macromolecular Substances, in 2007. Currently, she is associated with the Centre for Security, Information and Advanced Technologies, Faculty of Applied Informatics. Her research interests include modelling manufacturing processes of natural and synthetic polymers, analysis of thermal processes in building technology, studies of sensor system and wireless communication, and signal processing for motion monitoring. She is oriented toward computational and visualisation methods in thermographics, spatial modelling, and engineering. She serves as a reviewer for Springer, Elsevier, Wiley, and IEEE journals.

MICHAELA HONZÍRKOVÁ received the M.D. degree in general medicine from the Charles University, Prague. She is currently associated with Motol University Hospital, she is a member of the Czech Medical Association, and she is a member of Digital Signal and Image Processing Research Group, Department of Mathematics, Informatics and Cybernetics, UCT, Prague. Her research interests cover biomedical data acquisition, motion disorders treatment, image evaluation in dermatology, and diagnosis and treatment of skin diseases, biomedicine, biochemotheraphy, dermatology, and physiological data analysis. She received the certification of general medicine, in 2021.

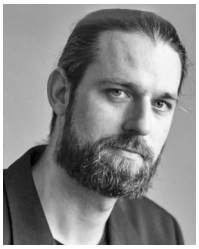

MARTIN SCHÄTZ received the Ph.D. degree in technical cybernetics from the University of Chemistry and Technology, Prague, Czech Republic, in 2021. He is a member of the Digital Signal and Image Processing Research Group with the Department of Mathematics, Informatics and Cybernetics, UCT. His professional experience includes bioimage analysis service in the open access Viničná Microscopy Core Facility of the Faculty of Science, Charles University, Prague. His research interests include information engineering, signal and image processing, computational methods of multidimensional data analysis, feature extraction, machine learning, and classification. Applications of his research include biomedicine, neurology, and physiological data processing.